Journal of Hazardous Materials 462 (2024) 132717

Contents lists available at ScienceDirect

Journal of Hazardous Materials

journal homepage: www.elsevier.com/locate/jhazmat

Research Paper

Nanoplastic impact on bone microenvironment: A snapshot from murine bone cells

Domenica Giannandrea [a,1], Marco Parolini [b,1], Valentina Citro [a], Beatrice De Felice [b], Alex Pezzotta [c], Nazanin Abazari [a], Natalia Platonova [a], Michela Sugni [b], Martina Chiu [d], Alessandro Villa [a], Elena Lesma [a], Raffaella Chiaramonte [a,1], Lavinia Casati [a,*,1]

[a] Department of Health Sciences, University of Milan, Italy
[b] Department of Environmental Science and Policy, University of Milan, Italy
[c] Department of Medical Biotechnology and Translational Medicine, University of Milan, Italy
[d] Department of Medicine and Surgery, University of Parma, Italy

HIGHLIGHTS

- Nanoplastic influence bone remodelling through oxidative stress.
- Nanoplastics enter in bone cells affecting their viability.
- Nanoplastics potentiate the osteoclastogenesis and impair the osteoblastogenesis
- Nanoplastics affect the inflammatory and osteoblastogenic pathways in bone cells

GRAPHICAL ABSTRACT

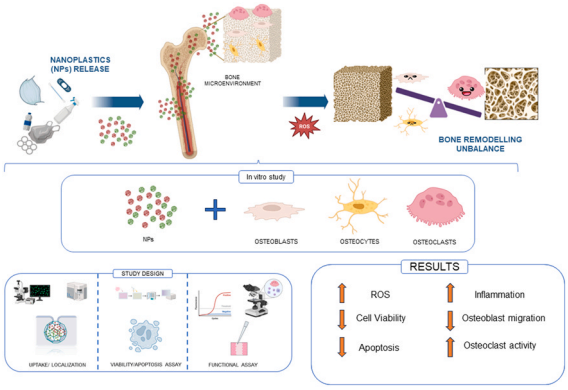

ARTICLE INFO

Editor: Karina S. B. Miglioranza

Keywords:
Nanoplastics
Bone remodeling
Oxydative stress
Osteoclastogenesis
Osteoblastogenesis

ABSTRACT

Our world is made of plastic. Plastic waste deeply affects our health entering the food chain. The degradation and/or fragmentation of plastics due to weathering processes result in the generation of nanoplastics (NPs). Only a few studies tested NPs effects on human health. NPs toxic actions are, in part, mediated by oxidative stress (OS) that, among its effects, affects bone remodeling. This study aimed to assess if NPs influence skeleton remodeling through OS. Murine bone cell cultures (MC3T3-E1 preosteoblasts, MLOY-4 osteocyte-like cells, and RAW264.7 pre-osteoclasts) were used to test the NPs detrimental effects on bone cells. NPs affect cell viability and induce ROS production and apoptosis (by caspase 3/7 activation) in pre-osteoblasts, osteocytes, and pre-osteoclasts. NPs impair the migration capability of pre-osteoblasts and potentiate the osteoclastogenesis of preosteoclasts. NPs affected the expression of genes related to inflammatory and osteoblastogenic pathways in pre-osteoblasts and osteocytes, related to the osteoclastogenic commitment of pre-osteoclasts. A better understanding of the impact

* Corresponding author.
E-mail address: lavinia.casati@unimi.it (L. Casati).
[1] These authors contribute equally

https://doi.org/10.1016/j.jhazmat.2023.132717
Received 9 August 2023; Received in revised form 27 September 2023; Accepted 3 October 2023
Available online 5 October 2023

of NPs on bone cell activities resulting in vivo in impaired bone turnover could give more information on the possible toxicity consequence of NPs on bone mass and the subsequent public health problems, such as bone disease.

1. Introduction

Plastics are synthetic or semisynthetic polymers with thermoplastic or thermostable properties. The production of plastics is increasing year by year, starting either from fossil or renewable sources. Plastic items are an active part of our everyday life, and for this reason, the production of these materials increased by 660% between 1976 and 2016, reaching 300 million tons (PlasticsEurope, 2022). The massive demand, production, and use of plastics, coupled with their inappropriate end-life management and disposal, have resulted in the contamination of both aquatic and terrestrial ecosystems worldwide [1]. For instance, in 2019, 25.9 Mt of plastic waste was generated In European countries (PlasticsEurope, 2022), and most of them accumulated in the environment [2].

The degradation and/or fragmentation of plastics due to weathering processes result in the generation of microplastics (MPs) and nanoplastics (NPs) [3]. Because of their size, MPs and NPs enter the food chain, potentially threatening human health (European Food Safety Authority (2017). Moreover, some recent studies have demonstrated that inhalation represents a crucial exposure pathway for MPs and NPs in humans [4].

A plastic particle can be considered "nano" if at least two of its dimensions are less than 100 nm [5], but a shared definition of NPs is still lacking [6]. Existing wastewater treatment processes fail to remove NPs [7]. The breakdown of larger plastic items, such as the fragmentation of synthetic fibers during clothes washing [8], is an additional source of MPs and NPs [9]. NPs may be carriers of chemical and biological contaminants, thus increasing their transport and uptake by organisms and further amplifying their toxicity [10].

MPs and NPs from synthetic textile fibers can persist up to five years in the air and can be transported by the wind from clothes drying in the open or numerous other sources; hence, inhalation is an important entry route for MPs and NPs which are potentially resuspended in the atmosphere and easily transported in the wind due to their low density and small size [4,11]. In addition, the current pandemic associated with COVID-19 and the wearing of single-use face masks is leading to the release of large quantities of polypropylene MPs with consequences for marine and terrestrial ecosystems and potential adverse effects on human health [12].

A recent study demonstrated the presence of NPs composed of polyethylene terephthalate, polystyrene, or polyethylene in the blood of human donors with a mean concentration of 1.6 μg total plastic particles/ml blood sample [13] and, also, for MPs, in human placenta samples [14]. Once NPs enter the human body, they are uptaken by cells through different routes (i.e. phagocytosis, endocytosis) [15]. NPs also penetrate bone marrow [16,17], disrupting hemopoietic activity and possibly the bone microenvironment. In vitro and in vivo studies indicated that NPs could severely impact the human body, including physical stress and damage, cell death, inflammation, and immune responses [18]. The environmental impact of NPs is an increasingly worrying problem for human health due to the large-scale growth of plastic production and its resistance to degradation.

Studies focused on the toxicity of NPs showed that they induce reactive oxygen species (ROS) overproduction and oxidative stress (OS) in experimental animal models [2,19,20], and human cell lines [21].

Among the negative impacts of ROS overproduction, the disruption of skeleton integrity is a major effect, particularly during aging [22]. In physiological conditions (naive), ROS affects the balance of critical processes in bone remodelling (resorption and deposition) [23]. Indeed, previous studies showed that OS resulting from excessive levels of ROS or dysfunction of antioxidant defence is involved in osteoporosis [24]. In mice, it has been reported that increased cellular OS induces low-turnover osteopenia [25] and that bone mass progressively declines in association with decreased antioxidant enzyme levels [26].

In a recent paper from our laboratory, ROS increase has been identified as a common mechanism of sex steroid deficiency and aging in bone homeostasis [27]. Moreover, sex steroid deficiency may accelerate the effects of aging on skeletal involution, partially mediated by epigenetic mechanism [27]. As NPs are considered potential inductors of oxidative stress, exposure to NPs could affect bone cell activities, thus disrupting bone accrual during childhood and increasing bone loss during aging.

A better understanding of the impact of NPs on bone cell activities could give the necessary information on the possible consequence of NPs-mediated toxicity on bone turnover and subsequent human health problems, including bone disease.

Although several invivo and invitro studies confirmed that the internalization of NPs results in the onset of an oxidative stress condition, coupled with the induction of apoptosis and the modulation of inflammatory markers, to the best of our knowledge, no studies have investigated the role of NPs in the bone microenvironment, which remains an unexplored research field. Thus, the present study aimed at investigating if NPs can induce an impact on healthy bone cells. In detail, we explored whether NPs may influence skeleton remodeling through OS, testing our hypothesis on bone cells (including cell cultures representing preosteoblasts, osteocyte-like cells, and pre-osteoclasts). Cell viability, apoptosis level, cellular differentiation, and transcriptomic profile were investigated after NPs exposure. Considering the consistency in the outcomes of previous experiments investigating the effects of NPs exposure on different cell types, we expect that bone cell can internalize NPs and experience an oxidative stress condition.

2. Experimental plan

2.1. Cell cultures & reagents

2.1.1. Cell cultures

Murine osteoblastic cell line from ATCC (cat. CRL-2593), MC3T3-E1, were seeded in High Glucose DMEM, (Euroclone, Italy), supplemented with 10% FBS (Euroclone, Italy), as previously reported [28]. We replaced culture medium twice a week and MC3T3-E1 cells were weekly trypsinized. Murine osteocyte-like cells, MLOY-4, were kindly provided by Dr. Romanello (Hospital “Santa Maria della Misericordia”, Udine, Italy). We coated plates of 10 mm with type I collagen. MLOY-4 cells were seeded as previously described [29]. The cells were trypsinized twice a week. RAW264.7 were seeded in High Glucose DMEM, (Euroclone, Italy), supplemented with 10% FBS (Euroclone, Italy). We replaced culture medium twice a week, and RAW264.7 were weekly trypsinized.

2.1.2. NPs treatment

Fluorescent, spherical polystyrene NPs (diameter 50 nm, Excitation/emission peaks of 468/508 nm (Green), 542/612 nm (Red), and 365/447 nm, aqueous solution 1% solids) were purchased by ThermoFisher Scientific. NPs were used following the manufacturer instruction. The range of treatments was from 1 μg/ml to 200 μg/ml, and the time of the cell exposure was from 4 h to 96 h, depending on the experimental plan. NPs were used to treat MC3T3-E1, MLOY-4, RAW264.7. For uptake experiments NPs green were used at 1–200 μg/ml for 48 h. For immunofluorescence experiments NPs red were used at 100 μg/ml, for 48 h.

For cell viability, Nitrite assay, NPs green were used at 1–200 μg/ml for 48 h. For Caspase activity and ROS production NPs red ere used at 1–200 μg/ml for 48 h. For the scratch assay NPs green were used at 10–100 μg/ml for 48 h. For the osteoclastogenic assay NPs green were used at 10 μg/ml for 48 h. For the transcriptomic analysis NPs green were used at 100 μg/ml for 48 h.

2.2. NPs localization

2.2.1. Immunofluorescence (MC3T3-E1, MLOY-4, RAW264.7 - NPs 100 μg/ml, 48 h)

MC3T3-E1 cells, MLOY-4, and RAW264.7 cells (5000 cells/well) were grown on 22-mm glass coverslips in 6-well plates. After treatment with NPs RED (100 μg/ml), the cells were fixed with 4% paraformaldehyde in 0.12 M sucrose, permeabilized with 0.1% TritonX100 in PBS for 5 min, and stained with DAPI for 5 min. We visualized the cells using an Axioplan fluorescence microscope.

2.2.2. NPs uptake (MC3T3-E1, MLOY-4, RAW264.7 - NPs 1–200 μg/ml, 4 h)

For the analysis of NPs uptake by flow cytometry, MC3T3-E1, MLOY-4, and RAW264.7 cells were seeded (50000) in 24-well plate. After 24 h, the monolayer was treated with increasing concentration (1, 10, 100 and 200 μg/ ml) of NPs emitting fluorescence at 612 nm if excited at 542 nm, for 4 h at 37 °C or 4 °C. The NPs incorporation was evaluated in the FITC channel at the FACS Verse.

2.3. Functional assay

2.3.1. Viability and death parameter

2.3.1.1. Cell viability assay (MC3T3-E1, MLOY-4, RAW264.7 - NPs 1–200 μg/ml, 48 h). We analyzed the MC3T3-E1, MLO-Y4, and RAW264.7 cellular viability, seeding the cells at the density of 5000–10,000 cells/well in 96 multiwell plates. We evaluated the cell viability using MTT test as previously reported [30].

2.3.1.2. Cas3-7 enzymatic activity (MC3T3-E1, MLOY-4, RAW264.7 - NPs 1–200 μg/ml, 48 h). The Caspase 3–7 activation, measured by using the Casp3/Casp7 Apoptosis Kit (Abnova kit), was evaluated as it is considered a reliable indicator of cell apoptosis. We followed the instruction of protocol manufacturer. Briefly, we seeded 5000 cells for well in 96 multiwell. To test the Caspase activity, the half of the medium of each well was replaced with 100 μl of caspase 3/7 substrate mixed with Assay buffer. The plate was incubated at 37 °C for 1 h in the dark. The plate was read with a fluorescence microplate reader at Ex/Em = 490/525 nm (ENSIGHT, Perkin Elmer).

2.3.2. Free radicals production

2.3.2.1. ROS production (MC3T3-E1, MLOY-4, RAW264.7 - NPs 1–200 μg/ml, 48 h). ROS production was measured using 5(6)-carboxy-2′,7-dichlorofluorescin diacetate (CM-DCFA, Sigma-Aldrich, 10 μM) as previously indicated [31]. Briefly, cells were seeded in black 96-well plates and cultured for 24 h. On the day of the experiment, the cells were pre-incubated with NPs for 48 h at increasing concentrations (starting from 1 μg/ml to 200 μg/ml). After adding CM-DCFA, DCF fluorescence was assessed with a spectrofluorophotometer (Victor™, PerkinElmer) at the excitation (485 nm) and emission (530 nm) wavelength.

2.3.2.2. Nitrite analysis (MC3T3-E1, MLOY-4, RAW264.7 - NPs 1–200 μg/ml, 48 h). Nitrite production was measured as a marker of nitrosative stress to investigate the contribution of both the radical species inducing oxidative stress. Nitrite assay was performed following manufacturer's protocol. Briefly, a standard curve was prepared starting from the stock solution of sodium nitrite 0,1 M. Cells were seeded in 96-well plates and cultured for 24 h 100 μl of supernatants were used for nitrite dosage. We added the Griess reagent previously mixed as reported by the manufacturer protocol (Panreac). Reaction was incubated at 37 °C for 15 min and samples were analyzed in a microplate reader at the absorbance of 550 nm.

2.3.3. Bone activity assay

2.3.3.1. Scratch wound healing assay (MC3T3-E1, NPs 10–100 μg/ml, 48 h). A linear scratch on confluent MC3T3-E1 cells was performed by using a sterile tip. We removed the cellular debris by washing with PBS, and then we incubated the cells in DMEM 1% FBS alone or in the presence of NPs for 48 h (see [32] for reference). Images were acquired immediately after the scratch (t0) and at various times after treatment (t24, and t48) using an Olympus U-CMAD3 phase-contrast microscope equipped with a Zeiss Axiocam ICc1 camera at a 4x magnification. As previously reported, the images were analyzed by using ImageJ software (NIH, USA) [33]. The covered area percentage was calculated for each experimental group by measuring the wound size at different times from treatment compared with the initial (t0) wound size considered as 100%.

2.3.3.2. Osteoclastogenic differentiation assay (RAW264.7, NPs 10 μg/ml, 48 h). As shown in our previous paper [34], RAW264.7 cells were seeded in a 24-well plate in 250 μl of DMEM supplemented with 10% FBS at a density of 2,5 × 104 cells/ well with or without 30 ng/ml RANKL and with or without 10 μg/ml NPs. The exposure with NPs lasted 48 h. After 7 days, RAW264.7 cells were fixed on the culture plates with citrate-acetone solution and stained for tartrate resistant acid phosphatase (TRAP kit, Sigma-Aldrich). Osteoclasts were identified and counted under light microscopy considering TRAP positive cells the ones with ≥ 3 nuclei. Representative images of TRAP positive osteoclasts were acquired with Olympus U-CMAD3 phase- contrast microscope equipped with a Zeiss Axiocam ICc1 camera at 4x magnification.

2.4. Transcriptomic profile analysis (MC3T3-E1, MLOY-4, RAW264.7 - NPs 100 μg/ml, 48 h)

Transcriptomic profile analysis was performed as reported in our previous study [27]. Briefly, total RNA from cells exposed to NPs was extracted using AURUM Column kit (Biorad). RNA pellet concentrations were assessed spectrophotometrically using microcuvette G1.0 in Eppendorf Biopohotometer.

For the PCR Prime Arrays we used the PCR arrays commercially available from SAB (Qiagen) and from Biorad. Following the instruction, we extracted the total mRNA using Biorad Mini kit. The quality of RNA was evaluated with electrophoresis. The samples were read at the spectrophotometer. Total RNA (1 μg) was retrotranscribed using iScript Advanced cDNA kit from Biorad. For the PRIME PCR we analyzed 10 μg of cDNA for well. We used both negative and positive control for PCR, as requested by the assay. The reaction was carried on QuantStudio Fast 5 (Thermofisher Scientific) using 20 μl of the total volume for each well. Q-PCR was run following the manufacturer protocol (Biorad).

2.5. Statistical analysis

We used GraphPad Prism8 software (GraphPad Software, USA) for all statistical analyses. The results are expressed as the mean ± SEM of at least 3 independent experiments (6 replicates for each experiment). Differences between groups were evaluated by one-way or two-way ANOVA followed by Bonferroni post-hoc test. Significance was set up at p-value lower than 0.05.

3. Results

To assess the effect of NPs on biological functions of bone cells, we used murine bone cell cultures (i.e., MC3T3-E1 preosteoblasts, osteocyte-like MLOY-4 cells, and RAW264.7 pre-osteoclasts) as experimental models. These cell lines were treated in a time course from 24 to 96 h with increasing concentrations of fluorescent, spherical polystyrene NPs (diameter 50 nm, concentration range 0.1–200 μg/ml). We tested cell viability, ROS level, and apoptosis by MTT, DCF, and fluorometric assay, respectively. Cellular morphology, as well as NPs localization and uptake, were also assessed. To investigate the effect of NPs on the bone remodeling process, we analyzed changes in the migration capability of MC3T3-E1 cells and the osteoclastogenic potential of RAW264.7 cells. Lastly, the transcriptomic profile of MC3T3-E1, MLOY-4, and RAW264.7 cells was evaluated.

3.1. Nanoplastics Localization and Uptake

The three cell lines were exposed to increasing NPs concentrations (1–200 μg/ml) according to the concentration range already used in in vitro studies [35]. The cellular uptake of NPs was evaluated by exposing for 4 h the cell lines to increasing concentrations of polystyrene NPs emitting fluorescence at 508 nm when excited at 468 nm. The internalization was analyzed at 37 ° and at 4 °C to verify the inhibition of uptake by flow cytometry in the FITC channel. For each cell line, we show the MFI (mean fluorescence intensity) in the panels A (Fig. 1) and the SSC (side scatter channel) parameters in the panels B (Fig. 1). The MFI indicates the shift of fluorescence of the cells positive for NPs, and SSC is an index of the complexity degree and granularity of the cell surface. In Fig. 1, we observed that in MC3T3-E1 cells, the MFI increases in a dose-dependent manner, indicating that the higher the concentration of NPs, the higher uptake of NPs in the cells. Additionally, the

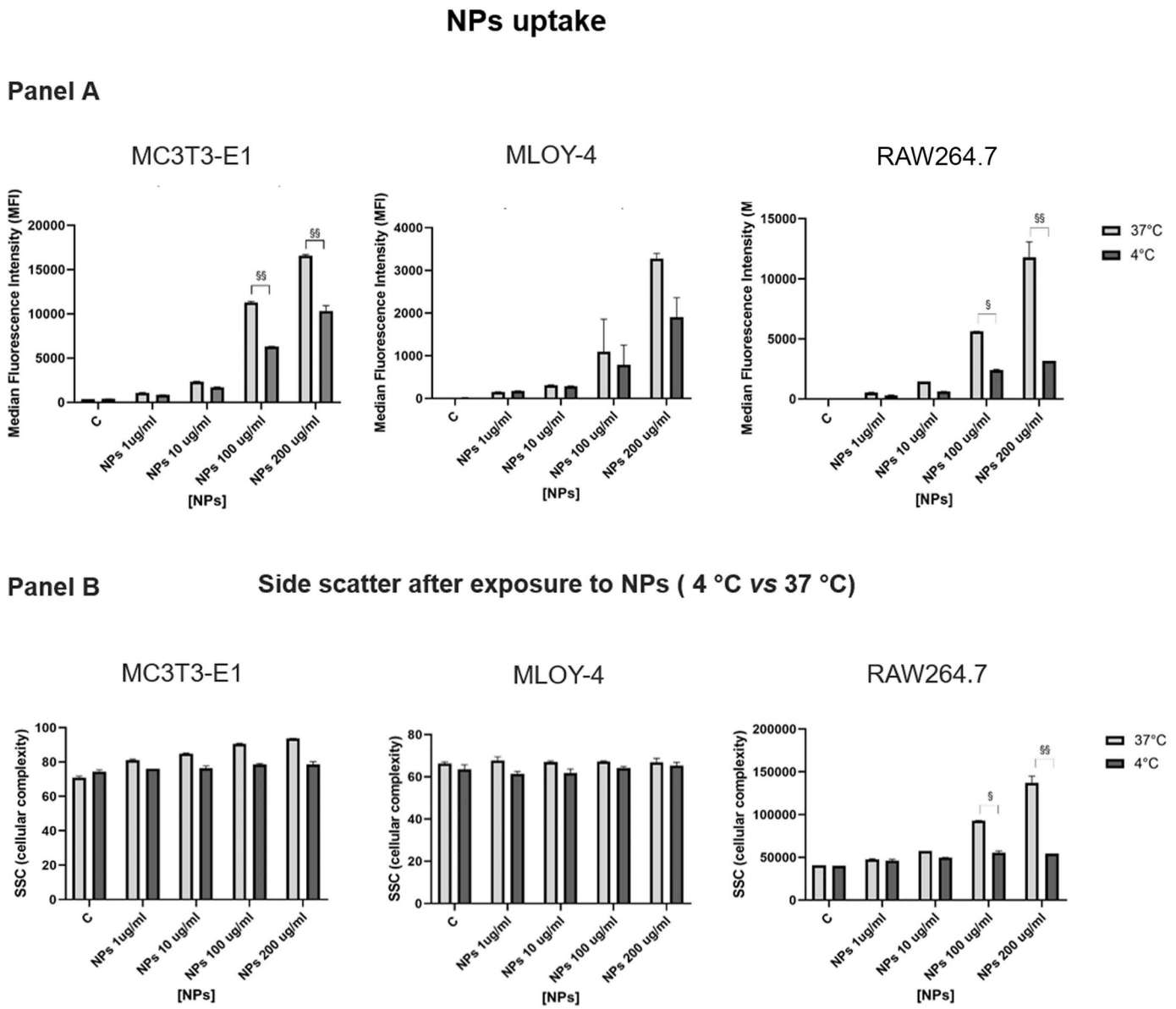

Fig. 1. Murine bone cells can uptake nanoplastics in a dose-dependent manner. MC3T3-E1, MLOY-4 and RAW264.7 cell lines were treated for 4 h at 37 °C and 4 °C with increasing concentrations of NPs (1–200 μg/ml) and the uptake was evaluated by flow cytometry analysing the median fluorescence intensity (MFI) in the FITC channel at FACS verse (panel A). For each cell line, changes in cell complexity assessed by the side scatter (SSC) channel parameter analysis were also analysed (panel B). The graphs report the mean (± SEM) of at least 3 independent experiments (6 replicates for each experiment). Statistical analysis was performed by two-way ANOVA followed by Bonferroni post-hoc test. 37 °C vs 4 °C: $ =$p < 0.05$; $$=$p < 0.01$.

significant decrease of MFI at 4 °C compared to 37 °C suggests that even though a passive uptake is present at high NPs concentrations, NPs route of access in these cells is at least partly controlled by the cell membrane. Finally, upon cell uptake, a slight change in cell complexity was observed by analyzing the SSC. In the osteocyte-like MLOY-4 cells, NPs uptake occurred with a similar trend, although no changes in SSC were associated with NPs exposure. Differently, the monocyte cell line RAW264.7 cells, displayed an increased control of NPs uptake with a more linear uptake of NPs at 37 °C and 4 °C. Also, the SSC parameter indicated a more marked change in cell complexity.

NPs localization within the cellular compartment was confirmed by microscope immunofluorescence after 48 h-exposure to 100 μg /ml polystyrene. In Fig. 2, results for MC3T3-E1, MLOY-4, and RAW264.7 cells are reported. The fluorescent signal associated with NPs was localized in the cytoplasm.

3.2. Nanoplastic effect on cell viability, apoptosis, and ROS production

To assess NP effect on cytotoxicity, we evaluated the cell viability by MTT assay, the caspase-3 activity related to the induction of the apoptotic process, and the ROS and nitrite production. The three cell lines were exposed to increasing NPs concentrations (from 1 to 200 μg/ml) according to concentration range already used in in-vitro studies [35]. The most effective time of exposure, 48 h, was set up with a time course (data not shown). As shown in Fig. 3**A**, the outcome on cell viability is different for the three cell lines. In particular, NPs caused a similar effect on mesenchymal cells (preosteoblasts and osteocytes), while it had a different action on macrophage-derived cells (pre-osteoclasts). NPs at the concentration of 100 μg/ml significantly reduced cell viability of MC3T3-E1 cells (around 20%), and caused a similar trend in MLOY-4 cells, even if more intense at the concentration of NPs of 200 μg/ml which induced the reduction of MLOY-4 cell

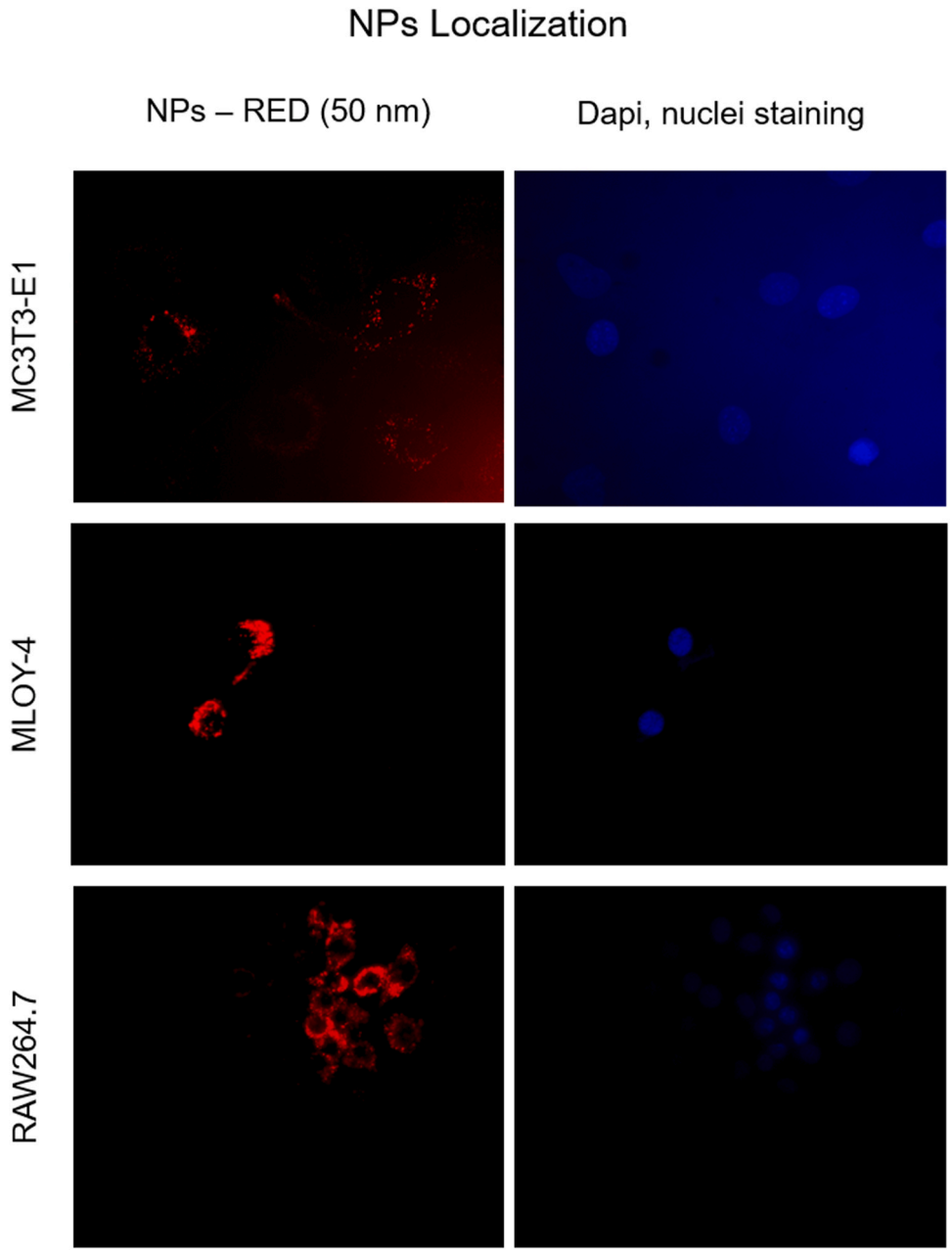

Fig. 2. NPs localize within the cellular compartment. MC3T3-E1, MLOY-4, and RAW264.7 cell lines were treated for 48 h with 100 μg/ml of NPs-RED and its cellular localization was assessed with an Axioplan fluorescence microscope. Red fluorescence: NPs; blue fluorescence: nuclei with DAPI (40x magnification).

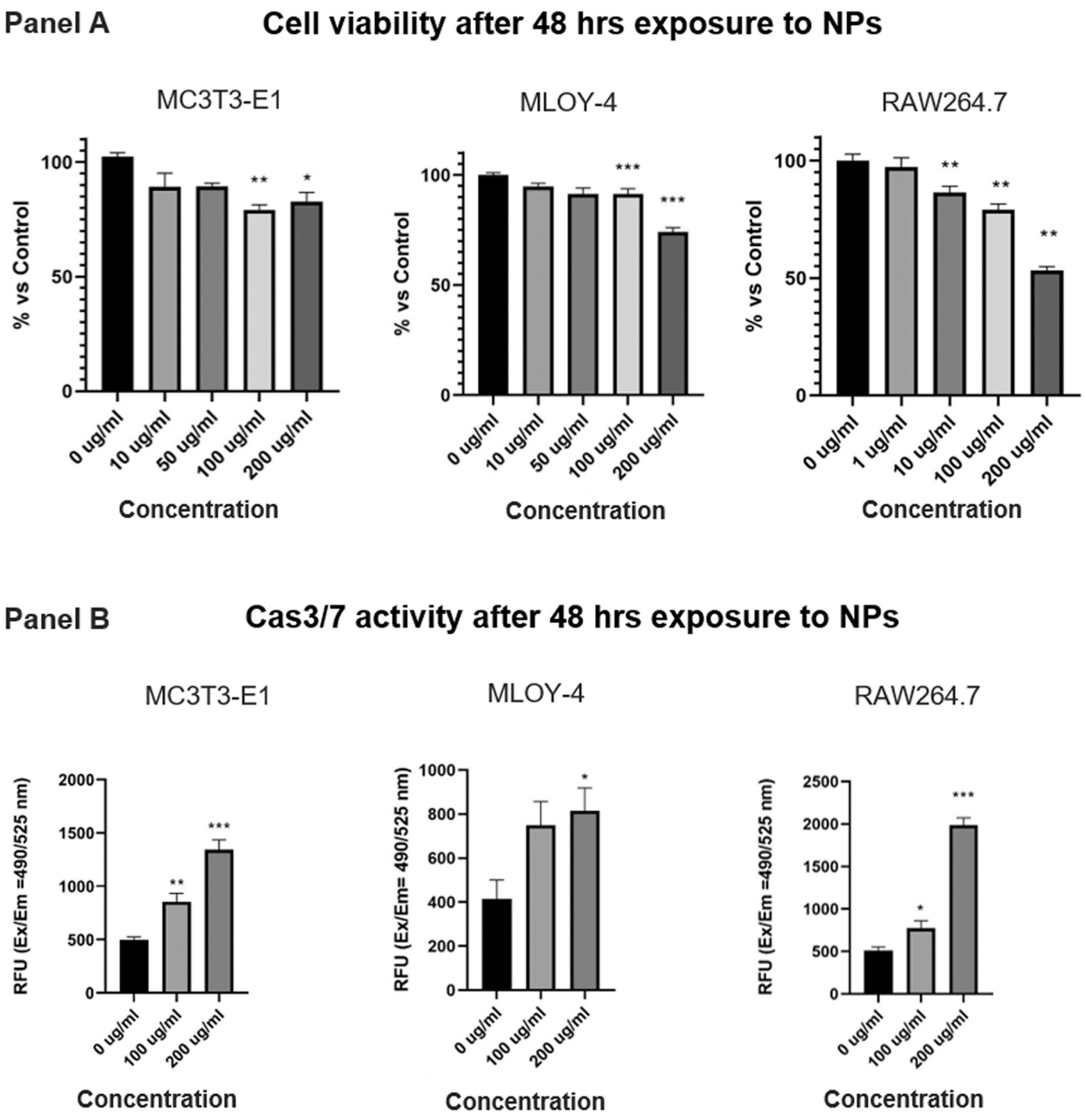

Fig. 3. Effect of NPs on the cell viability and apoptosis. MC3T3-E1, MLOY-4 and RAW264.7 cell lines were treated for 48 h with increasing concentrations of NPs (1–200 μg/ml). Cell viability was assessed by MTT assay (panel A) and apoptotic activity was performed by the enzymatic activity of caspase 3/7 by using a commercial kit from AbNova (panel B). The graphs report the mean (± SEM) of at least 3 independent experiments (6 replicates for each experiment) in which data are reported as the percentage vs control. Statistical analysis was performed by one way ANOVA followed by Bonferroni post-hoc test. Conditions vs control: * =$p < 0.05$; ** =$p < 0.01$; *** =$p < 0.001$.

viability around 35% compared to controls. RAW264.7 cells resulted to be more sensitive to NPs, indeed a statistically significant reduction of the cellular viability was observed at 10 μg/ml and an approximate decrease of 50% at the concentration of 200 μg/ml NPs. To assess if the effect of NPs on cell viability could be ascribed to an increase in apoptosis, we evaluated the apoptotic process through the enzymatic activity of caspase 3/7 after 48 h of NPs exposure. The results reported in Fig. 3**B** indicate that NPs induce the caspase 3/7 enzymatic activity with both concentrations, 100 and 200 μg/ml.

The assessment of radical oxygen production by DCFHDA assay and nitrite levels by Griess assay after 48 h of NPs exposure is reported in Fig. 4**A**. The two mesenchymal cell types (MC3T3-E1 and MLOY-4 cells) displayed similar ROS production, with a slight, but significant, increase (around 10%−15) at the higher NPs concentrations. On the contrary, as reported in Fig. 4**B**, in MC3T3-E1 cells, NPs induced nitrite production at a value around 4 μM, while MLOY-4 cells did not produce nitrites. The

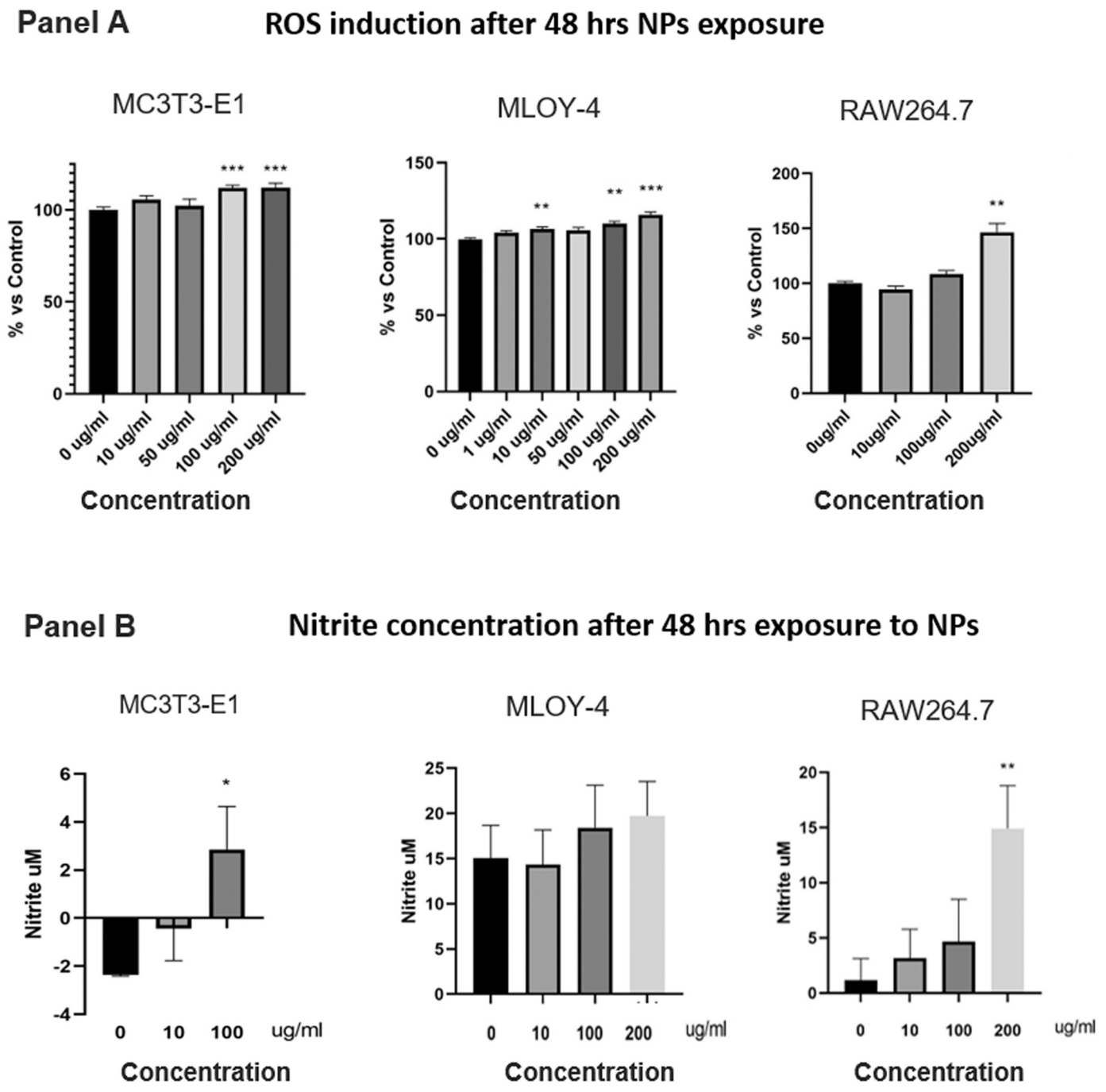

Fig. 4. NPs affect the ROS production in murine bone cell lines. MC3T3-E1, MLOY-4 and RAW264.7 cells were exposed for 48 h to increasing concentrations of NPs (1–200 μg/ml) and the radical oxygen production was assessed by DCFHDA assay (panel A), while nitrite levels by Griess assay (panel B). The graphs report the mean (± SEM) of at least 3 independent experiments (6 replicates for each experiment) showing the data as the percentage vs control. Statistical analysis was performed by ANOVA followed by Bonferroni post-hoc test. Conditions vs control: * =$p < 0.05$; ** =$p < 0.01$; *** =$p < 0.001$.

effects of NPs on RAW264.7 cells are more significant than those in MC3T3-E1 cells. RAW264.7 cells exhibit an increase of ROS production of 40% at NPs concentration of 200 μg/ml and an enhancement of nitrite release of ca. 15 μM, which is more than double in comparison to the control group.

3.3. Nanoplastics effect on bone cell biology

Osteoblast migration represents a key process in the physiological control of bone metabolism, including responses to mechanical loading [32]. As reported in our previous paper, impairment of the migratory potential of osteoblastic cells could also play a role in bone disease onset [27]. For this reason, we analysed the NPs effect on the migratory capability of MC3T3-E1 cells by using the scratch assay. As reported in Fig. 5, a pre-treatment of 48 h with NPs reduced the wound healing capability of MC3T3-E1 cells, after 24 h from scratch. This negative effect was observed only at the highest concentration of NPs (100 μg/ml).

As osteoclastogenesis is a fundamental prerequisite for bone remodelling, we investigated the role of NPs on osteoclast differentiation. For this purpose, tartrate-resistant acid phosphatase (TRAP) analysis was performed after a RANK-L-induced differentiation and exposure to 50 μg/ml of NPs. After 7 days of differentiation, $TRAP^{+}$ cells with

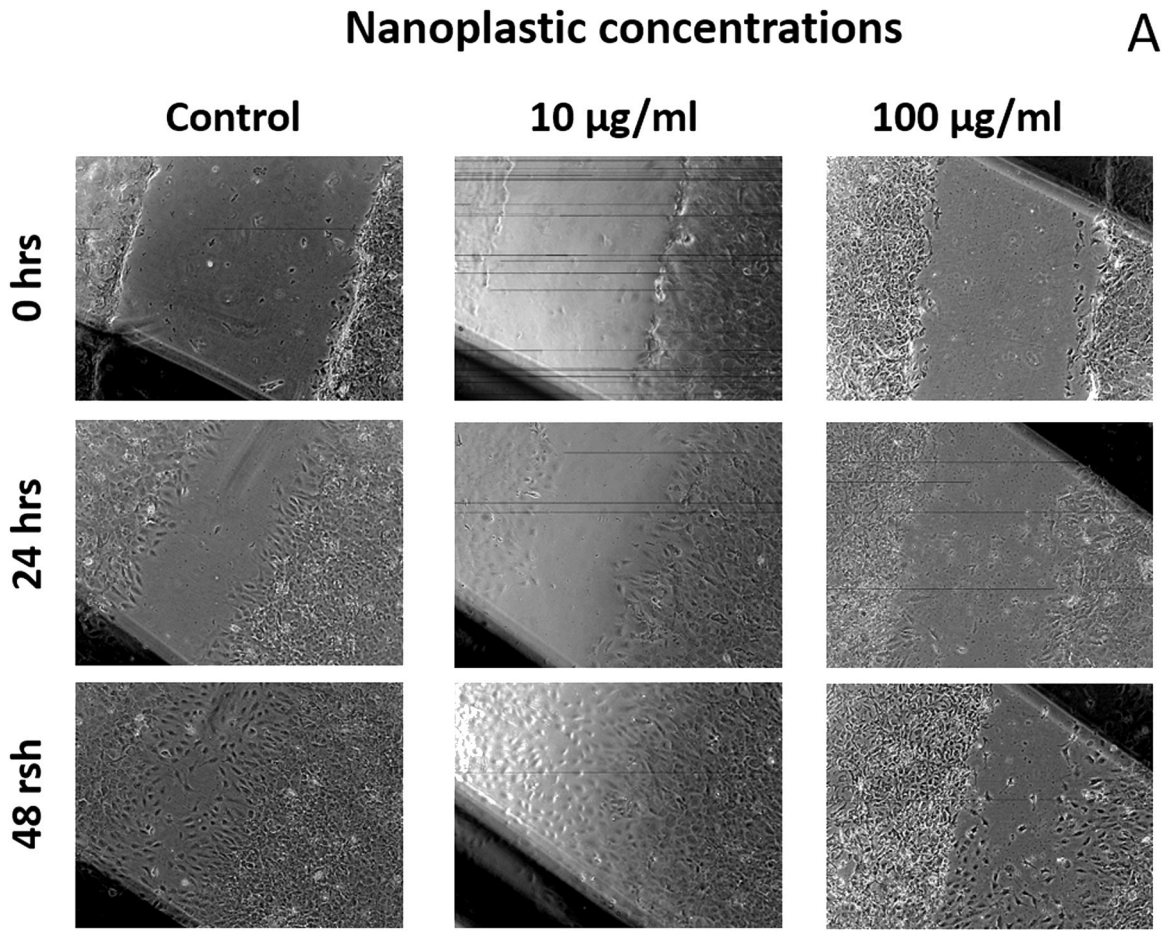

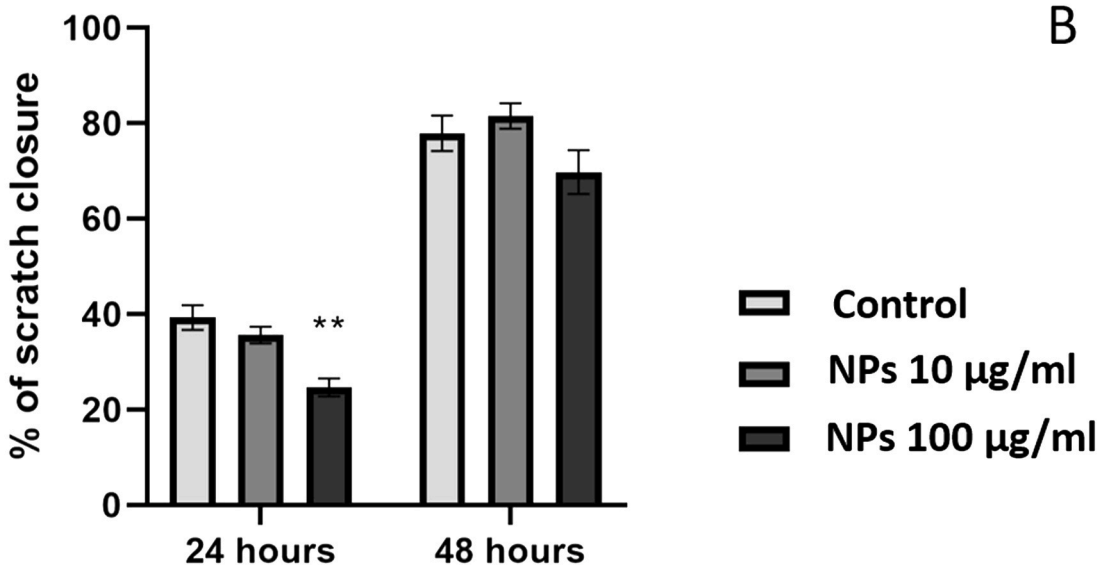

Fig. 5. NPs affect the migratory ability of MC3T3-E1 cells. The effect of NPs on the migratory ability of MC3T3-E1 cells, treated for 48 h with 10 and 100 µg/ml NPs, was evaluated by a wound healing assay assessed 24 h and 48 hoursafter the scratch (panel A). The graph (panel B) reports the mean (± SEM) of at least 3 independent experiments (6 replicates for each experiment) considering the data as the percentage vs control. Statistics analysis was performed by one way ANOVA followed by Bonferroni post-hoc test. Conditions vs control: ** =$p < 0.01$. Representative images reported above for each condition were acquired with Olympus U-CMAD3 phase-contrast microscope equipped with a Zeiss Axiocam ICc1 camera at a 4x magnification.

more than 3 nuclei were counted. As shown in Fig. 6, in the presence of a differentiation factor such as RANKL, NPs displayed an osteoclastogenic activity, increasing the number of osteoclasts as well as their size.

3.4. Transcriptomic Profile

To complete the landscape of the effect of NPs on bone cells, we performed a transcriptomic analysis on MC3T3-E1, MLOY-4, and RAW264.7 cells exposed to NPs (100 μg/ml) for 48 h by RT-PCR focusing on the profile of 88 genes involved in bone remodelling using a commercial PCR array for 88 genes putative involved in osteoporosis pathway.

Fig. 7 shows the profile of the genes affected after exposure to NPs in MC3T3-E1 cells. In detail, NPs significantly reduced the mRNA expression of the following genes *HSD11b1, TNFRSF11b,* and *IGF1*. Moreover, a decrease of mRNA expression of *IGFBP2* coupled with an increase of *IL-15* was observed, although not statistically significant. *HSD11b1* gene codes for hydroxysteroid 11-β dehydrogenase-1 enzyme, which is involved in converting cortisol into the inactive metabolite cortisone (Fig. 7A). *TNFSR11B*, also known as osteoprotegerin, is involved in inhibiting osteoclastogenesis (Fig. 7B). *IGF1* encodes for the insulin-like growth factor 1, a critical mediator of bone growth (Fig. 7C). *IGFBP2* encodes for Insulin-like growth factor binding protein 2, crucial for acquiring correct bone mass in mice (Fig. 7D). *IL-15* codes for a pro-inflammatory cytokine involved in osteoclastogenesis (panel E). The observed modulation of *IGF1, TNFSR11B1*, *IGFBP2,* and *IL-15* is consistent with the decrease of bone deposition and an increase in bone resorption.

Fig. 8 shows the modulation of genes affected by NPs in MLOY-4. Similarly to MC3T3-E1, NPs reduced the mRNA expression of *HSD11b1* (panel A). On the contrary, the gene expression of *Cnr2*(panel B), *CD40* (panel C), and *Nog* (panel D) increased. *Cnr2* encodes for Cannabinoid receptor type 2, *CD40* encodes for Tumor Necrosis Factor Receptor Superfamily Member 5, and *Nog* encodes for Noggin protein. *Cnr2, Nog,* and *CD40* are involved in the inflammatory process. *Nog*, in detail, is an inhibitor of BMP-4.

Fig. 9 shows the transcriptomic profile of genes affected by NPs in RAW264.7 cells. NPs treatment of RAW264.7 cells modulated the

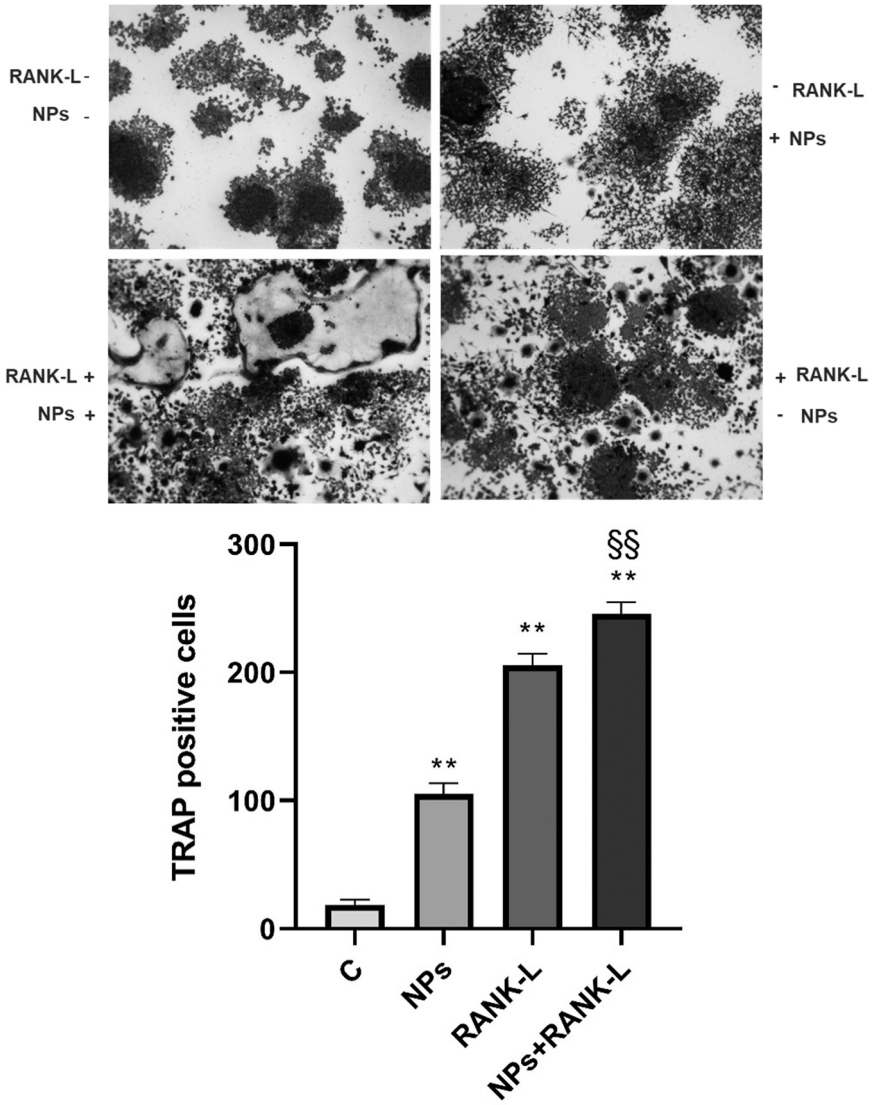

Fig. 6. NPs affect the osteoclastogenic ability of RAW264.7 cells. RAW264.7 cells were treated for 7 days with or without 50 μg/ml NPs after a RANK-L-induced differentiation. After 7 days of differentiation, $TRAP^+$ cells with ≥ 3 nuclei were identified and counted under light microscopy as TRAP positive cells. Graph shows the mean (± SEM) of at least 3 independent experiments (6 replicates for each experiment). Statistical analysis was performed by two-way ANOVA followed by Bonferroni post-hoc test. Conditions vs control: ** =$p < 0.01$; NPs+RANKL vs RANKL: $$=$p < 0.01$. Representative pictures of TRAP positive osteoclasts were acquired with Olympus U-CMAD3 phase- contrast microscope equipped with a Zeiss Axiocam ICc1 camera at 4x magnification.

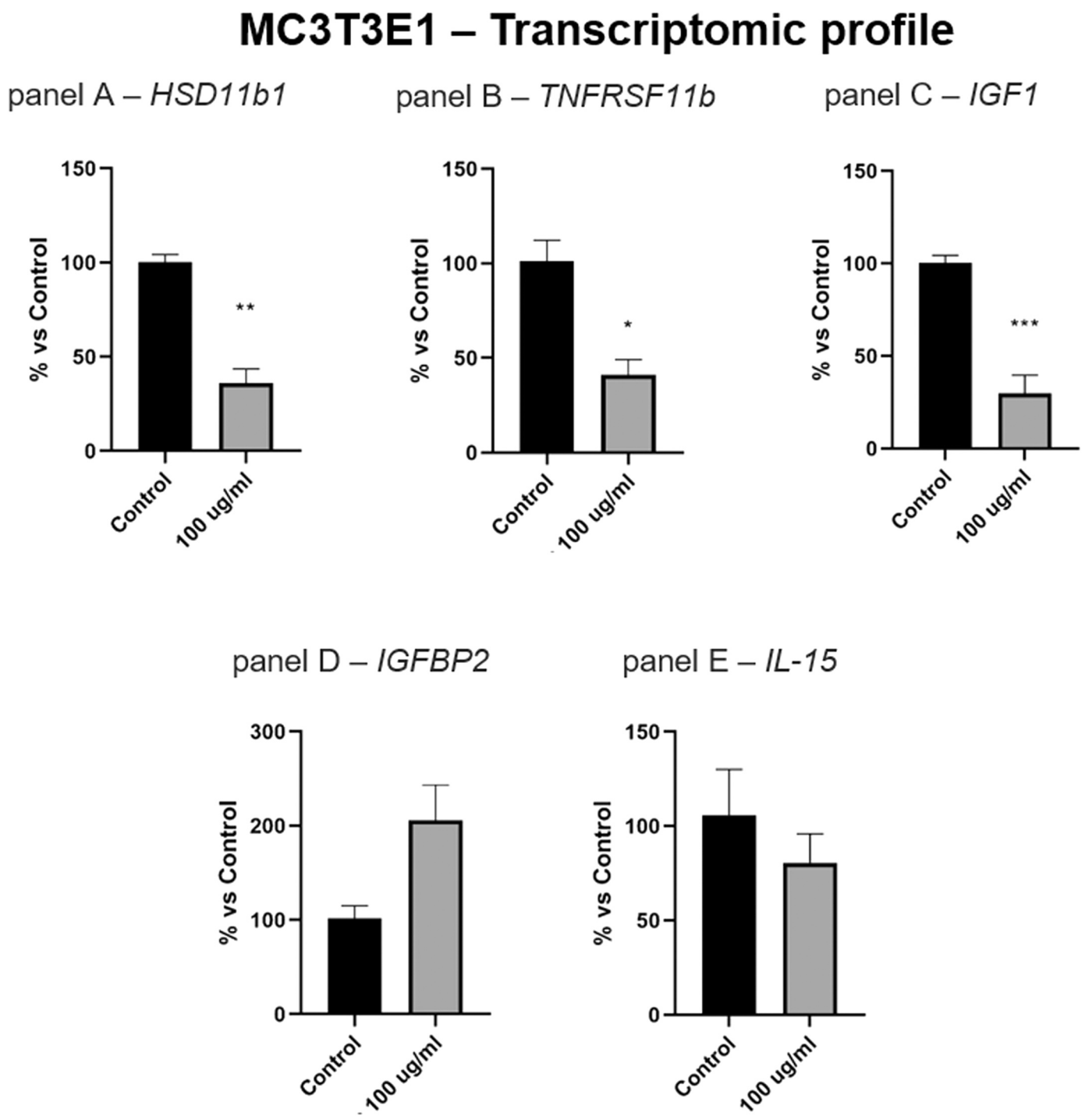

Fig. 7. Transcriptomic profile of MC3T3-E1 cells. The transcriptomic profile of MC3T3-E1 cells was assessed after 48 h of exposure to 100 μg/ml NPs by a commercial PCR array for 88 genes putative involved in osteoporosis pathway. The figure reports the modulation on the expression of the following genes: *HSD11b1* (panel A), *TNFRSF11b* (panel B), *IGF1* (panel C), *IGFBP2* (panel D) and *IL-15* (panel E). The graphs show the mean (± SEM) of at least 3 independent experiments (6 replicates for each experiment). Statistics analysis was performed by t-test. Conditions vs control: * =p < 0.05; ** =p < 0.01; *** =p < 0.001.

pattern of several genes related to osteoclastogenesis (panels A-G), indicating that these cells are susceptible to NPs. In detail, NPs induced the gene expression of *ACP5/TRAP*, encoding for the enzyme involved in bone matrix degradation and, thereby, a biomarker of active osteoclasts (panel A). As shown in Panel B, NPs induced the gene expression of *Alox15*, a negative regulator of bone mass acquisition. NPs also increased the gene expression of *IgtB3* encoding for the *Integrin Subunit Beta 3*, a key mediator of osteoclast-bone interaction (panel C). NPs exposure also induced the expression of *Mab21l2*, encoding for *Mab21-like-2* gene, a novel repressor of BMP-induced transcription (panel D). In Panel E, it is possible to observe that *Nog*, similarly to MLOY-4 cells, is induced by NPs. Panel F shows that NPs induced *Npy* mRNA, encoding for *Neuropeptide Y*, a negative osteogenesis regulator. In Fig. 9, panel G shows the gene expression of the *Twist1 gene*, a gene coding for a transcription factor involved in preparing metastatic niches in tumors, especially in bone districts. NPs induce the mRNA expression of *Twist1*. *Clcn7,* a gene coding for chloride voltage-gated channel 7, usually expressed in osteoclast ruffled board and osteopetrosis, is highly induced

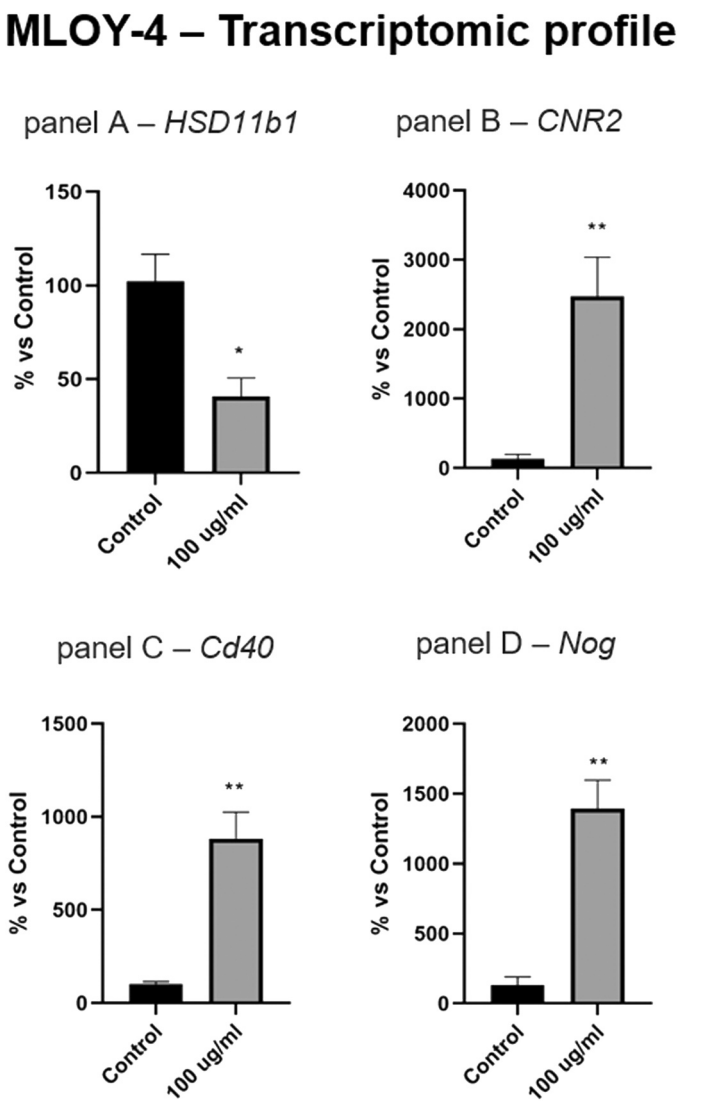

Fig. 8. Transcriptomic profile of MLOY-4 cells. The transcriptomic profile of MC3T3-E1 cells was assessed after 48 h exposure to 100 μg/ml NPs by a commercial PCR array for 88 genes putative involved in osteoporosis pathway. The figure reports the modulation on the expression of the following genes: *HSD11b1 (*panel A*), CNR2* (panel B), *Cd40* (panel C), *Nog* (panel D). The graphs show the mean (± SEM) of at least 3 independent experiments (6 replicates for each experiment). Statistical analysis was performed by Student t-test. Conditions vs control: * =p < 0.05; ** =p < 0.01; *** =p < 0.001.

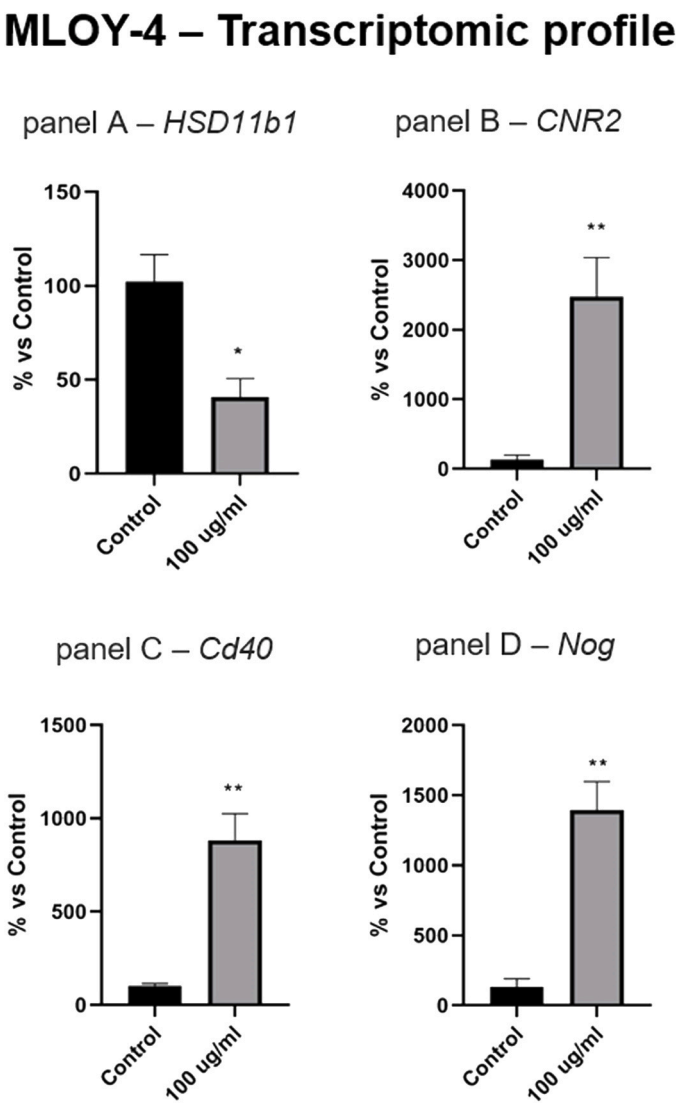

Fig. 9. Transcriptomic profile of RAW264.7 cells. The transcriptomic profile of RAW264.7 cells was assessed after 48 h exposure to 100 μg/ml NPs by a commercial PCR array for 88 genes putative involved in osteoporosis pathway. The figure reports the modulation on the expression of the following genes: *Acp5 (*panel A*), Alox15* (panel B), *Itgb3* (panel C), *Mab21l2* (panel D), *Nog* (panel E), *Nog* (panel E), *Npy* (panel F), *Twist1* (panel G), *Clcn7* (panel H). The graphs show the mean (± SEM) of at least 3 independent experiments (6 replicates for each experiment). Statistics analysis was performed by Student t-test. Conditions vs control: * =p < 0.05; ** =p < 0.01; *** =p < 0.001.

in RAW264.7 cells by NPs, as shown in Fig. 9, panel H.

4. Discussion

Our results indicate that NPs affect cell viability, induce ROS production (oxygen and nitrogen reactive species), and caspase 3/7 mediated apoptosis in all the cell lines tested. Moreover, NPs hampered the preosteoblast migration capability, which is directly involved in bone remodeling, and affected the gene expression of osteogenic pathways and related to inflammatory processes in the cell lines we used as biological models. In our opinion, the most relevant effect of NPs emerging from this study is the osteoclastogenic effects on the precursors of preosteoclasts, RAW264.7 cells. Indeed, NPs induced an increase of ROS levels and affected cell viability. Most importantly, NPs induced osteoclastogenesis, stimulating a transcriptomic profile consistent with osteoclastogenic differentiation.

Plastics represent one of our time's most important environmental pollutants. They are used in many activities and objects and strongly influence our daily lives in various ways. At the same time, these materials are also a significant source of environmental pollution to which human organism is exposed, unknowingly [36]. However, only a few studies analyze their true accumulation process and the mechanism of their toxicity at the cellular level [37]. A common mechanism involved in NPs cellular toxicity is the generation of free radical species. Several studies have highlighted NPs-induced molecular events such as free radical generation, activation of oxidative stress metabolism, lipid peroxidation, DNA damage, and signaling pathway activation. These mechanisms precede branched molecular changes that can lead to irreparable oxidative damage and inflammatory processes [38].

ROS are chemically active molecules involved in many biological processes.

When produced in excessive amounts, ROS are known to cause potentially toxic, mutagenic, or carcinogenic oxidative damage. Several

studies have shown that free radicals and ROS can affect the growth and function of osteoblasts and osteocytes [22–26]. The balance between the removal of old bone by osteoclasts and the synthesis of new bone by osteoblasts maintains the structural integrity of bone. If this mechanism is disrupted, it leads to various pathologies, such as osteoporosis or diseases that alter the bone environment.

NPs can cross biological membranes and interact with many intracellular sites [39]. The literature reports that NPs exposure reduce cell viability, leading to cell membrane instability, deterioration of cell organelles, ROS and nitrite generation, mitochondrial damage, and apoptotic and necrotic processes [40]. Our results clearly show that cells from the bone microenvironment can uptake NPs and cystosolic localization of the NPs in cellular compartment and is consistent with a previous study on the bone marrow demonstrating the accumulation of polystyrene MPs [16,17].

Besides cellular uptake, we show that NPs alter bone cells, often with a cell-specific effect. The alteration of the cellular morphology observed in SSC parameters linked to cell granularity, particularly for RAW264.7 cells and not for the others, could be likely related to the different derivation and the role of these cells. RAW264.7 cells are monocyte/macrophage-like cells originating from Abelson leukaemia virus transformed cell line derived from BALB/c mice. These cells are capable to perform pinocytosis and phagocytosis. Upon LPS stimulation, RAW264.7 cells increase nitric oxide (NO) production and enhance phagocytosis. NPs, inducing inflammatory/OS cues, could increase phagocytosis of NPs themselves, changing the granularity of the cells. Furthermore, the SSC parameter is related to a greater activation and maturation of human mononuclear phagocytes [41].

The reduction of cell viability was directly related to ROS production in the cells of bone component. Our previous studies indicate that osteocytes and osteoblasts are sensitive to ROS production [42]. Also, RAW264.7 cells are sensitive to OS [38]: our data clearly indicate a reduction of cell viability in line with the decrease of ROS production observed in RAW264.7 cells. The investigation of the role of NPs in the apoptosis pathway, indicated an increase of the Cas3/7 enzymatic activity in the all the three studied cell lines (MC3T3-E1, RAW264.7, MLOY-4 cells), although the sensitivity of the response is quite different among them. The apoptosis activation appears to be directly related to ROS production since apoptosis represents the main stress-induced cell death [43], so the differences found among the different cellular models is likely related to the difference of stimuli caused by the different ROS production induced by NPs in the three cell lines.

NPs induced an increase in osteoclastogenesis and a reduction of the level of genes involved in bone deposition. In detail, NPs increased differentiation of RAW264.7 cells toward osteoclast cells at the morphological and molecular levels. These could be related to the OS action, which acts toward osteoclastogenesis directions [29,44].

As highlighted in our previous paper [32], the analysis of osteoblast migratory activity could be considered as a new parameter for testing innovative therapeutical strateies for bone disease. We have already put in relation the effect of steroids and nutraceutical compounds in promoting migratory capability of preosteoblast MC3T3-E1 cells by Wnt/beta catenin pathway [27,32]. This pathway, crucial for the osteogenesis [45], is disrupted by OS [46]. NPs inducing OS affect also migratory capability of MC3T3-E1 cells.

Importantly, we observed an alteration in the transcriptomic profile, related to an induction towards a differentiated osteoclast phenotype in RAW264.7 cells, together to a disruption of the genes related to osteoblastogenesis in MC3T3-E1 cells and on inflammatory condition in the osteocyte-like MLOY-4 cells. The transcriptomic profile analyzed in MC3T3-E1 cells indicates an inhibition of the genes involved in osteoblastogenesis. NPs can affect the crosstalk between osteoblast and osteoclast by reducing OPG level (*TNFg1*), which is fundamental in controlling bone remodelling [47]. NPs are involved in reducing the gene expression of *IGF1* and *IGF2B*, which are critical mediators for bone growth and deposition, respectively [48,49]. From the literature, it is known the role of oxidative stress in counteracting osteoblastogenesis [22]. We found induction of the gene expression also of *IL15*, which is a widely expressed pro-inflammatory cytokine. Elevated IL15 receptor alpha (*IL15RA*) levels are found in the synovial fluid of patients affected by rheumatoid arthritis and other chronic inflammatory diseases that are associated with bone loss [50,51]. Moreover, *IL15* was shown to activate the osteoclasts mediated by NK cells [52].

The transcriptomic analysis of MLOY-4 cells after NPs exposure show an interesting profile related to the induction of inflammation and related to unhealthy aging. We observed induction of *Cnr2* and *Cd40,* which are both involved in the inflammatory process in the osteocytes [36,37].

In detail, *CD40* encodes for a transmembrane glycoprotein of around 48 kDa, belonging to TNSFR superfamily. *CD40* activates a pathway involved in the transcription of pro-inflammatory cytokines [36], whereas *Cnr2* is involved in the modulation of general inflammatory status [37]. In the transcriptomic profile of MLOY-4 cells, it was also found an alteration of *Nog* gene in common with RAW264.7 cells. Noggin protein can inhibit *BMP2* and *BMP-4* expression and can counteract bone mass deposition [53]. Studies from Sandri's group have highlighted that *Noggin* is involved in developing unhealthy aging and cachexia, and it is also derived from a reduction of bone deposition [54].

The NPs exposure in RAW264.7 cells shows a transcriptomic profile coherent with activation for these cells in the osteoclast direction. The genes induced by NPs are *Acp5*, *Alox15*, *Itgb3*, *Mab21l2*, *Nog*, *Npy*, *Twist1*, and *Ccln7*, all involved in osteoclastogenic pathways. As known, TRAP (tartrate-resistant acid phosphatase) is a key differentiation marker of osteoclastogenesis [55]. Alox15 is a lipoxygenase identified as a negative modulator of bone mineral density peak [56]. Itgb3 is the subunit b induced in osteoclasts during differentiation [57]. Mab21l2 was identified as a novel repressor of BMP-induced transcription [58]. As discussed above, Nog is involved in BMP inhibition [54]. The neuropeptide Npy is a multifunctional neuropeptide that participates in various physiological and pathological processes and is present in both the nerve system and bone tissue: of note, Npy negatively direct the osteogenesis [59,60]. Twist is a transcription factor that educates the metastatic niche in the bone [61] and its induction in osteoclasts could be related to a wider change involving the bone microenvironment. Clcn7 is a chloride channel expressed in the ruffled board of the osteoclasts, and it is a key target gene of bone resorption [62]. The fact that all these genes are induced by NPs exposure, indicates that NPs can induce an osteoclastogenic profile in RAW264.7 cells. All data derived from the three cell lines that resemble the bone components indicate an unbalance between bone deposition and resorption caused by NPs exposure in the bone microenvironment.

5. Conclusions

Our data first showed that NPs can be internalized into different types of murine bone cells, efficiently passing through membranes. Once in the cells, NPs can induce diverse detrimental effects on bone cells by modifying (increasing or inhibiting) specific functions. Specifically, NPs affected cell viability, induced ROS production and triggered the apoptotic process in pre-osteoblasts, osteocytes, and pre-osteoclasts, confirming that the mechanism of toxic action of NPs in cells is mediated by the onset of an oxidative stress condition. Moreover, NPs impaired the migration capability of pre-osteoblasts and potentiated the osteoclastogenesis of preosteoclasts. Finally, NPs exposure affected the gene expression profile of murine bone cell lines, modulating the expression of genes related to inflammatory process and of genes related to the osteoclastogenic commitment of pre-osteoclasts. Despite our findings, further studies are necessary to describe the complex landscape of NP effects on the bone microenvironment. Although our experiments showed that NPs exposure can affect the health status of different murine bone cells treated individually, considering their intimate and reciprocal interactions, assessing the effects of NPs in co-cultured bone

cells should be a priority. This approach allows to shed light on the effects on individual cell types subjected to paracrine interactions. Lastly, our experimental design should be replicated in normal human cells having pattern of proliferation/differentiation in culture more representative of the in vivo condition, to understand the link between NPs exposure, bone health and disease.

Funding

This work was supported by the Italian Minister of University and by European Union (NextGenerationEU, project code P2022RSWWF) and by Veronesi Foundation (project code FUV2021, 4340 and FUV 2020 3437).

CRediT authorship contribution statement

Domenica Giannandrea: Investigation, Writing – original draft, Writing – review & editing, Methodology. **Marco Parolini**: Investigation, Writing – original draft, Writing – review & editing, Visualization. **Valentina Citro**: Investigation. **Beatrice De Felice**: Writing – original draft. **Alex Pezzotta**: Writing – original draft. **Nazanin Abazari**: Investigation. **Natalia Platonova**: Writing – original draft, Visualization. **Michela Sugni:** Writing – original draft. **Martina Chiu**: Writing – review & editing. **Alessandro Villa**: Writing – review & editing. **Elena Lesma**: Writing – review & editing. **Raffaella Chiaramonte**: Supervision, Resource, Writing – review & editing. **Lavinia Casati**: Conceptualization, Investigation, Resource, Funding acquisition, Writing – original draft, Writing – review & editing.

Environmental Implications

Nanoplastics represent novel emerging contaminants in all the environmental compartments. Weathering, degradation, and fragmentation of large plastic debris can induce the production of nanoplastics. Because of their very small size, nanoplastics can interact with all living organisms, including humans, at all levels of biological organizations, entering the cells and altering different pathways. However, at present, the information concerning the toxicity of nanoplastics on conventional and non-conventional model organisms, as well as on humans is very limited. The present study enlarges the knowledge of nanoplastic toxicity, investigating diverse adverse effects induced on murine bone cells, a proxy of human cells, which can represent an additional target of these contaminants.

Declaration of Competing Interest

The authors declare that they have no known competing financial interests or personal relationships that could have appeared to influence the work reported in this paper.

Data Availability

Data will be made available on request.

References

[1] Rai, P.K., Lee, J., Brown, R.J.C., Kim, K.H., 2021. Environmental fate, ecotoxicity biomarkers, and potential health effects of micro- and nano-scale plastic contamination. J Hazard Mater 403, 123910.
[2] De Felice, B., Sugni, M., Casati, L., Parolini, M., 2022. Molecular, biochemical and behavioral responses of Daphnia magna under long-term exposure to polystyrene nanoplastics. Environ Int 164, 107264.
[3] Shen, M., Zhu, Y., Zhang, Y., Zeng, G., Wen, X., Yi, H., Ye, S., Ren, X., Song, B., 2019. Micro(nano)plastics: Unignorable vectors for organisms. Mar Pollut Bull 139, 328–331.
[4] Ortega, D.E., Cortés-Arriagada, D., 2023. Atmospheric microplastics and nanoplastics as vectors of primary air pollutants - a theoretical study on the polyethylene terephthalate (PET) case. Environ Pollut 318, 120860.
[5] Klaine, S.J., Koelmans, A.A., Horne, N., Carley, S., Handy, R.D., Kapustka, L., Nowack, B., von der Kammer, F., 2012. Paradigms to assess the environmental impact of manufactured nanomaterials. Environ Toxicol Chem 31 (1), 3–14.
[6] da Costa, J.P., Santos, P.S.M., Duarte, A.C., Rocha-Santos, T., 2016. Nano)plastics in the environment - sources, fates and effects. Sci Total Environ 566- 567, 15–26.
[7] Carr, S.A., Liu, J., Tesoro, A.G., 2016. Transport and fate of microplastic particles in wastewater treatment plants. Water Res 91, 174–182.
[8] Tosin, M., Weber, M., Siotto, M., Lott, C., Degli Innocenti, F., 2012. Laboratory test methods to determine the degradation of plastics in marine environmental conditions. Front Microbiol 3, 225.
[9] Eerkes-Medrano, D., Thompson, R.C., Aldridge, D.C., 2015. Microplastics in freshwater systems: a review of the emerging threats, identification of knowledge gaps and prioritisation of research needs. Water Res 75, 63–82.
[10] de Souza Machado, A.A., Kloas, W., Zarfl, C., Hempel, S., Rillig, M.C., 2018. Microplastics as an emerging threat to terrestrial ecosystems. Glob Chang Biol 24 (4), 1405–1416.
[11] Dris, R., Gasperi, J., Mirande, C., Mandin, C., Guerrouache, M., Langlois, V., Tassin, B., 2017. A first overview of textile fibers, including microplastics, in indoor and outdoor environments. Environ Pollut 221, 453–458.
[12] Lee, M., Kim, H., 2022. COVID-19 pandemic and microplastic pollution. Nanomater (Basel) 12 (5).
[13] Leslie, H.A., van Velzen, M.J.M., Brandsma, S.H., Vethaak, A.D., Garcia-Vallejo, J. J., Lamoree, M.H., 2022. Discovery and quantification of plastic particle pollution in human blood. Environ Int 163, 107199.
[14] Ragusa, A., Svelato, A., Santacroce, C., Catalano, P., Notarstefano, V., Carnevali, O., Papa, F., Rongioletti, M.C.A., Baiocco, F., Draghi, S., D'Amore, E., Rinaldo, D., Matta, M., Giorgini, E., 2021. Plasticenta: first evidence of microplastics in human placenta. Environ Int 146, 106274.
[15] Yee, M.S., Hii, L.W., Looi, C.K., Lim, W.M., Wong, S.F., Kok, Y.Y., Tan, B.K., Wong, C.Y., Leong, C.O., 2021. Impact of microplastics and nanoplastics on human health. Nanomater (Basel) 11 (2).
[16] Jani, P., Halbert, G.W., Langridge, J., Florence, A.T., 1990. Nanoparticle uptake by the rat gastrointestinal mucosa: quantitation and particle size dependency. J Pharm Pharm 42 (12), 821–826.
[17] Jing, J., Zhang, L., Han, L., Wang, J., Zhang, W., Liu, Z., Gao, A., 2022. Polystyrene micro-/nanoplastics induced hematopoietic damages via the crosstalk of gut microbiota, metabolites, and cytokines. Environ Int 161, 107131.
[18] Qiao, R., Sheng, C., Lu, Y., Zhang, Y., Ren, H., Lemos, B., 2019. Microplastics induce intestinal inflammation, oxidative stress, and disorders of metabolome and microbiome in zebrafish. Sci Total Environ 662, 246–253.
[19] Liu, Z., Yu, P., Cai, M., Wu, D., Zhang, M., Huang, Y., Zhao, Y., 2019. Polystyrene nanoplastic exposure induces immobilization, reproduction, and stress defense in the freshwater cladoceran Daphnia pulex. Chemosphere 215, 74–81.
[20] Parenti, C.C., Ghilardi, A., Della Torre, C., Magni, S., Del Giacco, L., Binelli, A., 2019. Evaluation of the infiltration of polystyrene nanobeads in zebrafish embryo tissues after short-term exposure and the related biochemical and behavioural effects. Environ Pollut 254(Pt A), 112947.
[21] Lehner, R., Weder, C., Petri-Fink, A., Rothen-Rutishauser, B., 2019. Emergence of nanoplastic in the environment and possible impact on human health. Environ Sci Technol 53 (4), 1748–1765.
[22] Almeida, M., O'Brien, C.A., 2013. Basic biology of skeletal aging: role of stress response pathways. J Gerontol A Biol Sci Med Sci 68 (10), 1197–1208.
[23] Dieci, E., Casati, L., Pagani, F., Celotti, F., Sibilia, V., 2014. Acylated and unacylated ghrelin protect MC3T3-E1 cells against tert-butyl hydroperoxide-induced oxidative injury: pharmacological characterization of ghrelin receptor and possible epigenetic involvement. Amino Acids 46 (7), 1715–1725.
[24] Almeida, M., Iyer, S., Martin-Millan, M., Bartell, S.M., Han, L., Ambrogini, E., Onal, M., Xiong, J., Weinstein, R.S., Jilka, R.L., O'Brien, C.A., Manolagas, S.C., 2013. Estrogen receptor-α signaling in osteoblast progenitors stimulates cortical bone accrual. J Clin Invest 123 (1), 394–404.
[25] Nojiri, H., Saita, Y., Morikawa, D., Kobayashi, K., Tsuda, C., Miyazaki, T., Saito, M., Marumo, K., Yonezawa, I., Kaneko, K., Shirasawa, T., Shimizu, T., 2011. Cytoplasmic superoxide causes bone fragility owing to low-turnover osteoporosis and impaired collagen cross-linking. J Bone Min Res 26 (11), 2682–2694.
[26] Almeida, M., Han, L., Martin-Millan, M., Plotkin, L.I., Stewart, S.A., Roberson, P.K., Kousteni, S., O'Brien, C.A., Bellido, T., Parfitt, A.M., Weinstein, R.S., Jilka, R.L., Manolagas, S.C., 2007. Skeletal involution by age-associated oxidative stress and its acceleration by loss of sex steroids. J Biol Chem 282 (37), 27285–27297.
[27] Sibilia, V., Bottai, D., Maggi, R., Pagani, F., Chiaramonte, R., Giannandrea, D., Citro, V., Platonova, N., Casati, L., 2021. Sex steroid regulation of oxidative stress in bone cells: an in vitro study. Int J Environ Res Public Health 18 (22).
[28] Mrak, E., Casati, L., Pagani, F., Rubinacci, A., Zarattini, G., Sibilia, V., 2015. Ghrelin increases beta-catenin level through protein Kinase A activation and regulates OPG expression in rat primary osteoblasts. Int J Endocrinol 2015, 547473.
[29] Casati, L., Pagani, F., Limonta, P., Vanetti, C., Stancari, G., Sibilia, V., 2020. Beneficial effects of δ-tocotrienol against oxidative stress in osteoblastic cells: studies on the mechanisms of action. Eur J Nutr 59 (5), 1975–1987.
[30] Casati, L., Pagani, F., Braga, P.C., Lo Scalzo, R., Sibilia, V., 2016. Nasunin, a new player in the field of osteoblast protection against oxidative stress. J Funct Foods 23, 474–484.
[31] Casati, L., Pagani, F., Fibiani, M., Lo Scalzo, R., Sibilia, V., 2018. Potential of delphinidin-3-rutinoside extracted from Solanum melongena L. as promoter of osteoblastic MC3T3-E1 function and antagonist of oxidative damage. Eur J Nutr.

[32] Casati, L., Pagani, F., Maggi, R., Ferrucci, F., Sibilia, V., 2020. Food for bone: evidence for a role for delta-tocotrienol in the physiological control of osteoblast migration. Int J Mol Sci 21 (13).
[33] Planz, V., Wang, J., Windbergs, M., 2018. Establishment of a cell-based wound healing assay for bio-relevant testing of wound therapeutics. J Pharm Toxicol Methods 89, 19–25.
[34] Giannandrea, D., Platonova, N., Colombo, M., Mazzola, M., Citro, V., Adami, R., Maltoni, F., Ancona, S., Dolo, V., Giusti, I., Basile, A., Pistocchi, A., Cantone, L., Bollati, V., Casati, L., Calzavara, E., Turrini, M., Lesma, E., Chiaramonte, R., 2022. Extracellular vesicles mediate the communication between multiple myeloma and bone marrow microenvironment in a NOTCH dependent way. Haematologica 107 (9), 2183–2194.
[35] Forte, M., Iachetta, G., Tussellino, M., Carotenuto, R., Prisco, M., De Falco, M., Laforgia, V., Valiante, S., 2016. Polystyrene nanoparticles internalization in human gastric adenocarcinoma cells. Toxicol Vitr 31, 126–136.
[36] Ma, D.Y., Clark, E.A., 2009. The role of CD40 and CD154/CD40L in dendritic cells. Semin Immunol 21 (5), 265–272.
[37] Sun, X., Cappelletti, M., Li, Y., Karp, C.L., Divanovic, S., Dey, S.K., 2014. Cnr2 deficiency confers resistance to inflammation-induced preterm birth in mice. Endocrinology 155 (10), 4006–4014.
[38] Zhang, Y., Fong, C.C., Wong, M.S., Tzang, C.H., Lai, W.P., Fong, W.F., Sui, S.F., Yang, M., 2005. Molecular mechanisms of survival and apoptosis in RAW 264.7 macrophages under oxidative stress. Apoptosis 10 (3), 545–556.
[39] Jiang, X., Weise, S., Hafner, M., Röcker, C., Zhang, F., Parak, W.J., Nienhaus, G.U., 2010. Quantitative analysis of the protein corona on FePt nanoparticles formed by transferrin binding. J R Soc Interface 7 (Suppl 1), S5–S13.
[40] He, H., Zheng, N., Song, Z., Kim, K.H., Yao, C., Zhang, R., Zhang, C., Huang, Y., Uckun, F.M., Cheng, J., Zhang, Y., Yin, L., 2016. Suppression of hepatic inflammation via systemic siRNA delivery by membrane-disruptive and endosomolytic helical polypeptide hybrid nanoparticles. ACS Nano 10 (2), 1859–1870.
[41] Dutertre, C.A., Becht, E., Irac, S.E., Khalilnezhad, A., Narang, V., Khalilnezhad, S., Ng, P.Y., van den Hoogen, L.L., Leong, J.Y., Lee, B., Chevrier, M., Zhang, X.M., Yong, P.J.A., Koh, G., Lum, J., Howland, S.W., Mok, E., Chen, J., Larbi, A., Tan, H. K.K., Lim, T.K.H., Karagianni, P., Tzioufas, A.G., Malleret, B., Brody, J., Albani, S., van Roon, J., Radstake, T., Newell, E.W., Ginhoux, F., 2019. Single-cell analysis of human mononuclear phagocytes reveals subset-defining markers and identifies circulating inflammatory dendritic cells. Immunity 51 (3), 573–589 e8.
[42] Casati, L., Pagani, F., Limonta, P., Vanetti, C., Stancari, G., Sibilia, V., 2020. Beneficial effects of delta-tocotrienol against oxidative stress in osteoblastic cells: studies on the mechanisms of action. Eur J Nutr 59 (5), 1975–1987.
[43] Farrell, L., Puig-Barbe, A., Haque, M.I., Amcheslavsky, A., Yu, M., Bergmann, A., Fan, Y., 2022. Actin remodeling mediates ROS production and JNK activation to drive apoptosis-induced proliferation. PLoS Genet 18 (12), e1010533.
[44] Almeida, M., Laurent, M.R., Dubois, V., Claessens, F., O'Brien, C.A., Bouillon, R., Vanderschueren, D., Manolagas, S.C., 2017. Estrogens and androgens in skeletal physiology and pathophysiology. Physiol Rev 97 (1), 135–187.
[45] McGonnell, I.M., Grigoriadis, A.E., Lam, E.W., Price, J.S., Sunters, A., 2012. A specific role for phosphoinositide 3-kinase and AKT in osteoblasts? Front Endocrinol (Lausanne) 3, 88.
[46] Wang, B., Shravah, J., Luo, H., Raedschelders, K., Chen, D.D., Ansley, D.M., 2009. Propofol protects against hydrogen peroxide-induced injury in cardiac H9c2 cells via Akt activation and Bcl-2 up-regulation. Biochem Biophys Res Commun 389 (1), 105–111.
[47] Tobeiha, M., Moghadasian, M.H., Amin, N., Jafarnejad, S., 2020. RANKL/RANK/OPG pathway: a mechanism involved in exercise-induced bone remodeling. Biomed Res Int 2020, 6910312.
[48] Locatelli, V., Bianchi, V.E., 2014. Effect of GH/IGF-1 on bone metabolism and osteoporsosis. Int J Endocrinol 2014, 235060.
[49] Xi, G., Wai, C., DeMambro, V., Rosen, C.J., Clemmons, D.R., 2014. IGFBP-2 directly stimulates osteoblast differentiation. J Bone Min Res 29 (11), 2427–2438.
[50] Loro, E., Ramaswamy, G., Chandra, A., Tseng, W.J., Mishra, M.K., Shore, E.M., Khurana, T.S., 2017. IL15RA is required for osteoblast function and bone mineralization. Bone 103, 20–30.
[51] Santos Savio, A., Machado Diaz, A.C., Chico Capote, A., Miranda Navarro, J., Rodríguez Alvarez, Y., Bringas Pérez, R., Estévez del Toro, M., Guillen Nieto, G.E., 2015. Differential expression of pro-inflammatory cytokines IL-15Ralpha, IL-15, IL-6 and TNFalpha in synovial fluid from rheumatoid arthritis patients. BMC Musculoskelet Disord 16, 51.
[52] Feng, S., Madsen, S.H., Viller, N.N., Neutzsky-Wulff, A.V., Geisler, C., Karlsson, L., Söderström, K., 2015. Interleukin-15-activated natural killer cells kill autologous osteoclasts via LFA-1, DNAM-1 and TRAIL, and inhibit osteoclast-mediated bone erosion in vitro. Immunology 145 (3), 367–379.
[53] Zaidi, M., Yuen, T., Sun, L., Rosen, C.J., 2018. Regulation of skeletal homeostasis. Endocr Rev 39 (5), 701–718.
[54] Sartori, R., Hagg, A., Zampieri, S., Armani, A., Winbanks, C.E., Viana, L.R., Haidar, M., Watt, K.I., Qian, H., Pezzini, C., Zanganeh, P., Turner, B.J., Larsson, A., Zanchettin, G., Pierobon, E.S., Moletta, L., Valmasoni, M., Ponzoni, A., Attar, S., Da Dalt, G., Sperti, C., Kustermann, M., Thomson, R.E., Larsson, L., Loveland, K.L., Costelli, P., Megighian, A., Merigliano, S., Penna, F., Gregorevic, P., Sandri, M., 2021. Perturbed BMP signaling and denervation promote muscle wasting in cancer cachexia. Sci Transl Med 13 (605).
[55] Reithmeier, A., Norgård, M., Ek-Rylander, B., Näreoja, T., Andersson, G., 2020. Cathepsin K regulates localization and secretion of Tartrate-Resistant Acid Phosphatase (TRAP) in TRAP-overexpressing MDA-MB-231 breast cancer cells. BMC Mol Cell Biol 21 (1), 15.
[56] Klein, R.F., Allard, J., Avnur, Z., Nikolcheva, T., Rotstein, D., Carlos, A.S., Shea, M., Waters, R.V., Belknap, J.K., Peltz, G., Orwoll, E.S., 2004. Regulation of bone mass in mice by the lipoxygenase gene Alox15. Science 303 (5655), 229–232.
[57] Purdue, P.E., Crotti, T.N., Shen, Z., Swantek, J., Li, J., Hill, J., Hanidu, A., Dimock, J., Nabozny, G., Goldring, S.R., McHugh, K.P., 2014. Comprehensive profiling analysis of actively resorbing osteoclasts identifies critical signaling pathways regulated by bone substrate. Sci Rep 4, 7595.
[58] Benisch, P., Schilling, T., Klein-Hitpass, L., Frey, S.P., Seefried, L., Raaijmakers, N., Krug, M., Regensburger, M., Zeck, S., Schinke, T., Amling, M., Ebert, R., Jakob, F., 2012. The transcriptional profile of mesenchymal stem cell populations in primary osteoporosis is distinct and shows overexpression of osteogenic inhibitors. PLoS One 7 (9), e45142.
[59] Chen, Q.C., Zhang, Y., 2022. The role of NPY in the regulation of bone metabolism. Front Endocrinol (Lausanne) 13, 833485.
[60] Matic, I., Matthews, B.G., Kizivat, T., Igwe, J.C., Marijanovic, I., Ruohonen, S.T., Savontaus, E., Adams, D.J., Kalajzic, I., 2012. Bone-specific overexpression of NPY modulates osteogenesis. J Musculoskelet Neuron Inter 12 (4), 209–218.
[61] Croset, M., Goehrig, D., Frackowiak, A., Bonnelye, E., Ansieau, S., Puisieux, A., Clézardin, P., 2014. TWIST1 expression in breast cancer cells facilitates bone metastasis formation. J Bone Min Res 29 (8), 1886–1899.
[62] Meadows, N.A., Sharma, S.M., Faulkner, G.J., Ostrowski, M.C., Hume, D.A., Cassady, A.I., 2007. The expression of Clcn7 and Ostm1 in osteoclasts is coregulated by microphthalmia transcription factor. J Biol Chem 282 (3), 1891–1904.